Available online at www.sciencedirect.com

ScienceDirect

Ceramics International 40 (2014) 2581–2584

CERAMICS INTERNATIONAL

www.elsevier.com/locate/ceramint

Green and red upconversion luminescence of Er^{3+}-doped $K_{0.5}Na_{0.5}NbO_3$ ceramics

Haiqin Sun[a,b,c,*], Qiwei Zhang[c], Xusheng Wang[a,b,1], Mu Gu[a,b,c,2]

[a]*Shanghai Key Laboratory of Special Artificial Microstructure Materials and Technology, Department of Physics, Tongji University, 1239 Siping Road, 20092 Shanghai, PR China*

[b]*Functional Materials Research Laboratory, Tongji University, Siping Road 1239, Shanghai 200092, PR China*

[c]*School of Rare Earth, Inner Mongolia University of Science and Technology, 014010 Baotou, PR China*

Received 27 June 2013; received in revised form 13 October 2013; accepted 21 October 2013
Available online 31 October 2013

Abstract

Er^{3+} doped $K_{0.5}Na_{0.5}NbO_3$ (KNN) lead-free piezoelectric ceramics were synthesized by the solid-state reaction method. The upconversion emission properties of Er^{3+} doped KNN ceramics were investigated as a function of Er^{3+} concentration and incident pumping power intensity. Bright green (~555 nm) and red (670 nm) upconversion emission bands were obtained under 980 nm excitation at room temperature, which are attributed to ($^2H_{11/2}$, $^4S_{3/2}$)→$^4I_{15/2}$ and $^4F_{9/2}$→$^4I_{15/2}$ transitions, respectively. The upconversion emission intensity can be adjusted by changing Er^{3+} concentration, and the mechanism of upconversion processes involve not only a two-photon absorption but also a three-photon absorption. In addition to the admirable intrinsic piezoelectric properties of KNN, this kind of material may have potential application as a multifunctional device by integrating its upconversion and piezoelectric property.

Keywords: A. Powders: solid state reaction and sintering; C. Optical properties; D. Perovskites

1. Introduction

Upconversion (UC) describes the nonlinear optical process, namely, an UC material can generate one higher-energy visible (400–750 nm) or near-infrared (NIR, 750 nm to 3 μm) photon from every two or more lower-energy (NIR) photons. Since its concept was first proposed in 1959 [1], UC materials have received a great deal of attention in diverse research fields, not only because of their fundamental scientific importance but also for their potential application in short-wavelength lasers, fluorescent labeling, temperature sensors, color displays, data storage, biological imaging, medical therapy, and solar cells, and so on [2–5]. Nowdays, the UC emission has been observed and studied in many rare-earth doped bulk materials. Among the rare-earth ions, the trivalent erbium ion (Er^{3+}) is the most popular as one of the most efficient ions for UC due to its favorable energy level structure with $^4I_{15/2}$→$^4I_{11/2}$ transition in the near-infrared(NIR) spectral region which can be conveniently excited by commercial low-cost near-infrared laser diodes (LD) [5–8].

Sodium potassium niobate $K_{0.5}Na_{0.5}NbO_3$ (KNN) is a prototype material of lead-free alkaline-transition metal ferroelectrics with an $A^{1+}B^{5+}O_3^{2+}$ perovskite structure, which is a solid solution of ferroelectric $KNbO_3$ and antiferroelectric $NaNbO_3$ by the ratio of 1:1. Due to its high Curie temperature (420 °C) and large electromechanical coupling factors, the KNN is considered as a promising candidate for lead-free piezoelectric ceramics to replace the widely used lead-based materials due to Pb toxicity [9–11]. As we know, rare earth elements are frequently used in piezoelectric materials to improve the electrical properties. Meanwhile, some rare earth ions can also act as the activator ions of luminescent materials

*Corresponding author at: Shanghai Key Laboratory of Special Artificial Microstructure Materials and Technology, Department of Physics, Tongji University, 1239 Siping Road, 20092 Shanghai, PR China.
Tel.: +86 21 65980544.
E-mail addresses: 09zqw@tongji.edu.cn (H. Sun), xs-wang@tongji.edu.cn (X. Wang), mgu@tongji.edu.cn (M. Gu).
[1]Fax: +86 21 65985179.
[2]Fax: +86 21 65980219.

0272-8842/$ - see front matter © 2013 Elsevier Ltd and Techna Group S.r.l. All rights reserved.
http://dx.doi.org/10.1016/j.ceramint.2013.10.089

because of the special intra-4f layer in rare earth ions [12,13]. In the last several years, the $BaTiO_3$ [14] and $Bi_{0.5}Na_{0.5}TiO_3$ [15] materials with perovskite ABO_3 structure have been confirmed to possess UC luminescence properties by Er^{3+} ions doping. In our preliminary work, superior photoluminescence properties in Pr^{3+} ions doped KNN host has been successfully observed [16]. Thus, we believe that some rare-earth ions such as Er^{3+}, Yb^{3+}, Ho^{3+} doped KNN host may exhibit UC emission properties. Hence, the aim of this study is to report our investigation results on the synthesis and UC luminescence of Er^{3+} doped KNN ceramics.

2. Experiments

The Er^{3+} doped KNN ceramics were designed according to the formula of $(K_{0.5}Na_{0.5})Nb_{1-x}Er_xO_{3-x/2}$ (where $0 \le x \le 0.05$, abbreviated as KNN:xEr) and synthesized using a conventional solid-state reaction technique. The starting materials, K_2CO_3 (99.0%, Alfa Aesar), Na_2CO_3 (Tianjin Chemical Reagent, 99.95%), Nb_2O_5 (99.5%, Alfa Aesar), and Er_2O_3 (99.99%, Sinopharm), were weighed and ball milled with addition of alcohol. The mixed powders were calcined in an alumina crucible at 880 °C for 6 h in air. Then, they were remilled. The remilled powders were granulated with polyvinyl alcohol (PVA) and pressed into pellets. Finally, the green pellets were sintered at 1100–1200 °C for 4 h in air. The conventional X-ray diffraction (XRD, Bruker D8 Advanced, Germany) was employed for phase identification. The up-conversion spectra were measured by a power controllable 980 nm laser diode (LD). The visible emissions from the samples were detected by a monochromator with an attached photomultiplier tube. All the measurements were performed at the room temperature.

3. Results and discussion

Fig. 1 shows the X-ray diffraction (XRD) patterns of the representative sintered KNN:xEr (x=0, 0.005, 0.01, 0.03) ceramic pellets. The samples with low Er levels ($x \le 1$ mol%) are all single-phase ABO_3 perovskite structure, whereas those with high Er levels ($x > 1$ mol%) exhibit a second phase. This observation means that, when $x \le 1$ mol%, the Er^{3+} doped KNN samples possess the $(K_{0.5}Na_{0.5})NbO_3$ orthorhombic perovskite phase and Er^{3+} ions have diffused into the lattice of the KNN host, but when, Er^{3+} cannot diffuse fully into the lattice and resulting in the impurity.

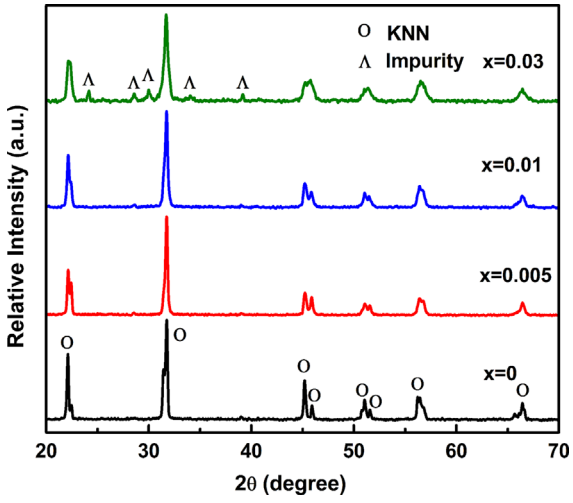

Fig. 1. The XRD patterns of the sintered KNN:xEr (x=0, 0.005, 0.01, 0.03) ceramic pellets.

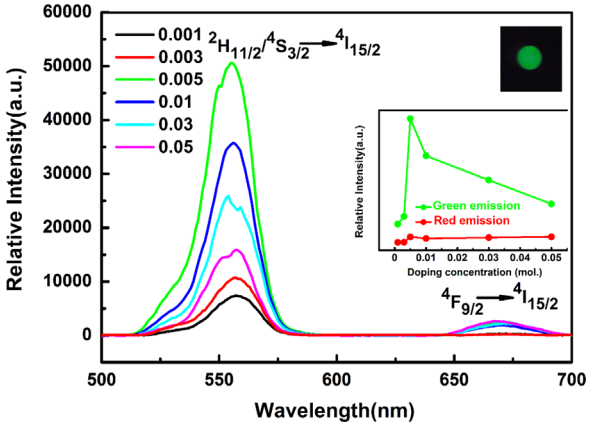

Fig. 2. Upconversion emission spectra of the sintered KNN:xEr ceramic pellets under 980 nm excitation. Inset: the photograph of KNN:0.005Er sample and the fluorescence intensity of the green and red emission versus the Er^{3+} doping concentration. (For interpretation of the references to color in this figure, the reader is referred to the web version of this article.)

The room temperature UC emission spectra of the sintered KNN:xEr ceramic pellets doped with different Er concentrations under 980 nm LD excitation are presented in Fig. 2. It can be clearly seen that the typical UC emission consists of two parts: a very strong green emission band at 510–590 nm and a relatively weak red emission band at 645–695 nm, wherein the green band centered at 555 nm is attributed to the intra 4f–4f electronic transition ($^2H_{11/2}$, $^4S_{3/2}$)→$^4I_{15/2}$ of Er^{3+} ions, the red emission band centered at about 670 nm attributed to another intra 4f–4f electronic transition $^4F_{9/2}$→$^4I_{15/2}$ of Er^{3+} ions. All emission bands are in accordance with the results reported in literatures for other hosts doping by Er^{3+} ions [7,8,15]. In addition, from the figure, it also can be seen that the green emission intensities at 555 nm are more predominant than the red emission at 670 nm for all KNN:xEr ceramics, and the intensity of the former is about 20 times as strong as that of the latter. Thus, the room temperature UC emission of the samples pumped by 980 nm LD can be easily observed by the naked eyes and exhibits very bright green color. The photograph of the typical KNN:0.005Er sample under 980 nm excitation is shown in the inset of Fig. 2.

The UC luminescence properties are highly dependent on the activator concentration. In order to study this relationship, a series of samples with the formula of KNN:xEr (x=0.001, 0.003, 0.005, 0.01, 0.03, 0.05) ceramics have been prepared. The variations of the fluorescence intensity of the green (~555 nm) and red (~670 nm) emission versus Er^{3+} doping concentration are presented in the inset of Fig. 2. As the doping concentration increases, the green emission intensity shows a strong concentration-quenching effect [17]: firstly it

increases as the value of x increases and reaches to its maximum at $x=0.005$, then decreases with further increasing the amount of Er doping, which is different from the variations of the red one exhibiting a continuous increasing trend with the Er^{3+} doping concentration. The 4f–4f transitions arising from the forced electric dipole are parity forbidden and become partially allowed as the ion is situated at the low-symmetry site [18]. When a small amount of Er ions are introduced into the KNN host, the inequivalence substitution-induced defects can reduce the symmetry of the crystal structure of KNN host, then form luminescence centers in the matrix, and the number of luminescence centers increases as the dopant increases, which is beneficial to the luminescence emission. However, when the Er^{3+} concentrations excess some certain value, more and more defects and impurity phase will gather near the grain boundaries, and participate in the phonon relaxation process, then reduce the possibility of recombination radiation of luminescent center. Simultaneously, too many luminescence centers will shorten the distance between Pr^{3+} ions, leading to the enhancement of cross relaxation (CR) process, thereby significantly weaken the up-conversion process.

In the UC processes, the visible output intensity is proportional to the nth power of the NIR excitation intensity, i.e., $I_{up} \propto (P)^n$, where I_{up} and P represent the UC emission and pumping power intensity of the LD, respectively, and n is the number of NIR photons producing an visible UC photon. Calculating the slope of a double-logarithmic plot of UC emission intensity versus incident excitation power is a common method used to investigate the UC mechanism and the number of photons involved in the UC process. Fig. 3 shows the dependence of the UC intensities of the bands in the green ($(^2H_{11/2}, {}^4S_{3/2}) \rightarrow {}^4I_{15/2}$) and red ($^4F_{9/2} \rightarrow {}^4I_{15/2}$) regions on the pumping power intensity of the 980 nm laser for the sintered KNN:0.005Er sample. The slopes n of the two curves were 2.11 and 2.42, respectively. These results indicated that in the process of the green and red emission, two NIR excitation photons were required to produce one UC photon (two-photon absorption). Especially, there may be also involved in three-photon absorption in the process of red emission due to its slope value equal to 2.42.

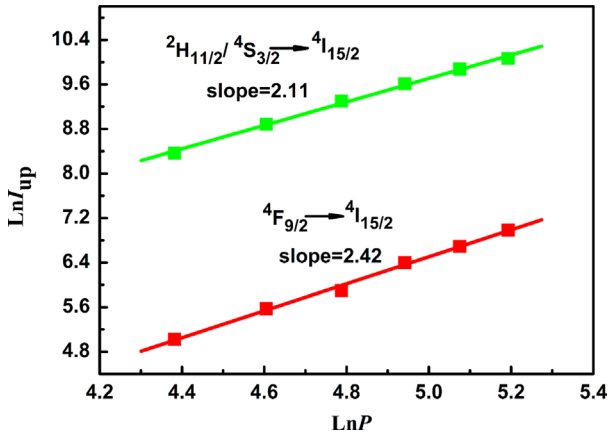

Fig. 3. The dependence of the UC intensities on the pumping power intensity of KNN:0.005Er samples in a logarithmic diagram. (For interpretation of the references to color in this figure, the reader is referred to the web version of this article.)

Fig. 4 sketches a typical energy-level diagram of Er^{3+} as well as the probable UC mechanisms accounting for the green and red emissions under 980 nm excitation. A UC luminescence process mainly consists of several parts: ground state absorption (GSA), excited state absorption (ESA), radiative transition, multiphonon relaxation and energy transfer upconversion (ET). As shown in Fig. 4, under the excitation of 980 nm light, Er^{3+} ions absorbs a 980 nm photon and are excited initially from the ground state $^4I_{15/2}$ to $^4I_{11/2}$ state in GSA process ($^4I_{15/2}$ + a photon $\rightarrow {}^4I_{11/2}$). Then, the Er^{3+} ions absorbs a photon again and are further excited to $^4F_{7/2}$ from the $^4I_{11/2}$ state via ESA process ($^4I_{11/2}$ + a photon $\rightarrow {}^4F_{7/2}$). Subsequently, the Er^{3+} ions at $^4F_{7/2}$ state then decays to the mixed state $^2H_{11/2} + {}^4S_{3/2}$ and $^4F_{9/2}$ state by multiphonon relaxation, relaxed to the ground state with radiative transition of green ($(^2H_{11/2}, {}^4S_{3/2}) \rightarrow {}^4I_{15/2}$) and red ($^4F_{9/2} \rightarrow {}^4I_{15/2}$) emission bands, respectively. The above mechanism is called a two-photo process, which is in agreement with the UC emissions in other Er^{3+} doped samples [6,8,15,18]. Additionally, it is suggested that the ET between two close Er^{3+} ions also takes place and plays a significant role in the upconversion emission. As shown in Fig. 4, the Er^{3+} ions in the $^4I_{11/2}$ state relax to the ground state through nonradiative relaxation and simultaneously transfer its energy to the neighboring Er^{3+} ions (also in $^4I_{11/2}$ state), promoting the latter to $^4F_{7/2}$ state. When the $^4F_{7/2}$ state is populated, consecutive multiphonon relaxation processes populate the mixed $^2H_{11/2} + {}^4S_{3/2}$ and $^4F_{9/2}$ states. Thus, the UC emissions are enhanced through the process of ET accompanied with EAS. Nevertheless, the cross-relaxation (CR) process: $^2H_{11/2} + {}^4S_{3/2} \rightarrow {}^4I_{9/2}$ and $^4I_{15/2} \rightarrow {}^4I_{13/2}$ would take place at a higher Er^{3+} doping. As a result, levels $^4I_{9/2}$ and $^4I_{13/2}$ become populated, as shown in Fig. 4. Then, the Er^{3+} ions at $^4I_{9/2}$ will populate to the lower states $^4I_{11/2}$ and $^4I_{13/2}$ by nonradiative relaxation processes or decaying radiatively to the ground state, while, the Er^{3+} ions at $^4I_{13/2}$ could not only decay radiatively to the ground state but also follow an UC promotion above the $^4F_{9/2}$ state through the ET process ($^4I_{13/2} + {}^4I_{11/2}$) $\rightarrow$ ($^4F_{9/2} + {}^4I_{15/2}$) among neighboring Er^{3+} interacting with each other. Once the ET process occurs, it will bring about an enhancement of red emission from the $^4F_{9/2}$

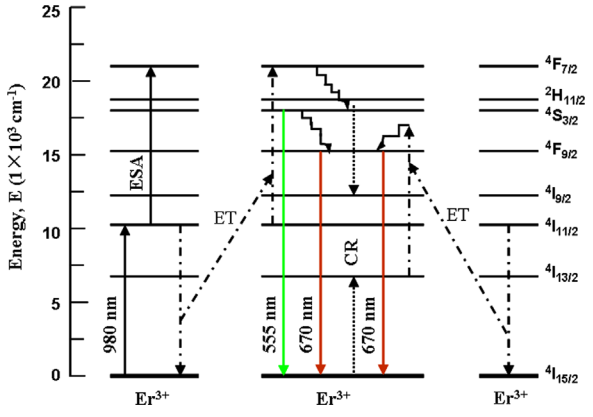

Fig. 4. Energy-level diagram of Er^{3+} ion as well as the probable upconversion mechanisms.

state and a quenching increase of the green emission from the mixed $^2H_{11/2}+{}^4S_{3/2}$ state with increasing Er^{3+} concentration. This phenomenon is well consistent with the observed variation of UC intensity curve of green and red emission for KNN:*x*Er UC phosphor presented in Fig. 2 as reported by other researchers [15]. Because the population of the $^4F_{9/2}$ state can be caused by both multiphoton relaxation from the $^4S_{3/2}$ state and ET process from the neighboring Er^{3+} ions, so, when doping level of Er^{3+} in KNN host is high enough (>0.005 mol), with the increase of Er^{3+} content, the UC emission intensity of the red band enhanced while the green band quenched rapidly. It is also confirmed that the excitation intensity-dependent data of the $^4F_{9/2}$ state for 0.005 mol Er^{3+} doped KNN sample in Fig. 3 were a combination of a two-photon and a three-photon process. Thus, the enhanced emissions for the red band in KNN:Er can be considered as the combined mechanism of CR and ET. It suggests that the red or green emission can be adjusted by the Er^{3+} concentration.

4. Conclusions

The green (555 nm) and red (670 nm) UC emission of Er^{3+} doped KNN ceramics were prepared by the traditional solid state reaction method. Their fluorescence properties were studied as a function of Er^{3+} concentration and incident pumping power intensity. The strong green and weak red bands were obtained under the 980 nm excitation at room temperature, which correspond to the radiative transitions from mixed states $^2H_{11/2}$, $^4S_{3/2}$ and $^4F_{9/2}$ to the ground state $^4I_{15/2}$, respectively. The dependence of the UC intensities on the pumping power intensity suggests that the green emission occurs via a two-photon process while the red emission involves not only a two-photon absorption but also a three-photon absorption. With a low Er^{3+} concentration, the green and red emissions were both enhanced. However, with a higher Er^{3+} concentration, the red emission was still enhanced, while the green emission quenched because of the CR+ETU processes. This results indicate that it is possible to tune the ratio of red to green emission by adjusting the Er^{3+} concentration. The KNN possess. Thus, the Er^{3+} doped KNN may take an important role in many fields as a multifunctional material with considering the admirable piezoelectric properties of the KNN.

Acknowledgments

This work was supported by the Natural Science Foundation of China (Nos. 51072136 and 50932007) and China Postdoctoral Science Foundation (2013M540384).

References

[1] N. Bloembergen, Solid state infrared quantum counters, Phys. Rev. Lett. 2 (3) (1959) 84–85.
[2] F. Auzel, Upconversion and anti-Stokes processes with f and d ions in solids, Chem. Rev. 104 (2004) 139–173.
[3] B.E. Cohen, Beyond fluorescence, Nature 467 (2010) 407–408.
[4] G. Wang, Q. Peng, Y. Li, Lanthanide-doped nanocrystals: synthesis, optical–magnetic properties, and applications, Acc. Chem. Res. 44 (2011) 322–332.
[5] S. Sergeyev, S. Popov, Excitation back transfer in a statistical model for upconversion in Er-doped fibres, J. Eur. Opt. Soc. Rap. Public 2 (2007) 07027.
[6] N. Rakov, C.B. De Araujo, Y. Messaddeq, M.A. Aegerter, Avalanche upconversion in Er^{3+} doped fluoroindate glass, Appl. Phys. Lett. 70 (1997) 3084–3086.
[7] F. Vetrone, J.C. Boyer, J.A. Capobianco, A. Speghini, M. Bettinelli, Significance of Yb^{3+} concentration on the upconversion mechanisms in codoped Y_2O_3:Er^{3+}, Yb^{3+} nanocrystals, J. Appl. Phys. 96 (2004) 661–667.
[8] B. Dong, X.S. Xu, X.J. Wang, T. Yang, Y.Y. He, Infrared-to-visible upconversion emissions and thermometric applications of Er^{3+}-doped Al_2O_3, Appl. Phys. B 89 (2007) 281–284.
[9] L. Egerton, D.M. Dillon, Piezoelectric and dielectric properties of ceramics in the system potassium–sodium niobate, J. Am. Ceram. Soc. 42 (9) (1959) 438–442.
[10] H.Y. Park, C.W. Ahn, H.C. Song, J.H. Lee, S. Nahm, Microstructure and piezoelectric properties of $0.95(Na_{0.5}K_{0.5})NbO_3$–$0.05BaTiO_3$ ceramics, Appl. Phys. Lett. 89 (2006) 062906.
[11] Y. Saito, H. Takao, T. Tani, T. Nonoyama, K. Takatori, T. Homma, T. Nagaya, M. Nakamura, Lead-free piezoceramics, Nature 432 (2004) 84–87.
[12] K.B. Ruan, X.M. Chen, T. Liang, G.H. Wu, D.H. Bao, Photoluminescence and electrical properties of highly transparent $(Bi,Eu)_4Ti_3O_{12}$ ferroelectric thin films on indium-tin-oxide-coated glass substrates, J. Appl. Phys. 103 (2008) 074101.
[13] H.Q. Sun, D.F. Peng, X.S. Wang, M.M. Tang, Q.W. Zhang, X. Yao, Strong redemission in Pr doped $(Bi_{0.5}Na_{0.5})TiO_3$ ferroelectric ceramics, J. Appl. Phys. 110 (2011) 016102.
[14] H. Zhang, C. Kam, Y. Zhou, X. Han, S. Buddhudu, Y. Lam, Visible upconversion luminescence in Er^{3+}:$BaTiO_3$ nanocrystals, Opt. Mater. 15 (1) (2000) 47–50.
[15] S. Chen, M.J. Wu, L.Q. An, Y.X. Li, S.W. Wang, Strong green and red upconversion emission in Er^{3+}-doped $Na_{1/2}Bi_{1/2}TiO_3$ ceramics, J. Am. Ceram. Soc. 90 (2) (2007) 664–666.
[16] H.Q. Sun, D.F. Peng, X.S. Wang, M.M. Tang, Q.W. Zhang, X. Yao, Green and red emission for $(K_{0.5}Na_{0.5})NbO_3$:Pr ceramics, J. Appl. Phys. 111 (2012) 046102.
[17] L.H. Spangler, B. Farris, E.D. Filer, N.P. Barnes, A computational study of host effects on Er^{3+} upconversion and self-quenching efficiency in ten garnets, J. Appl. Phys. 79 (2) (1996) 573–577.
[18] A. Patra, C.S. Friend, R. Kapoor, P.N. Prasad, Effect of crystal nature on upconversion luminescence in Er^{3+}:ZrO_2 nanocrystals, Appl. Phys. Lett. 83 (2) (2003) 284–286.